

# Imidazole Polymers Derived from Ionic Liquid 4-Vinylimidazolium Monomers: Their Synthesis and Thermal and Dielectric Properties

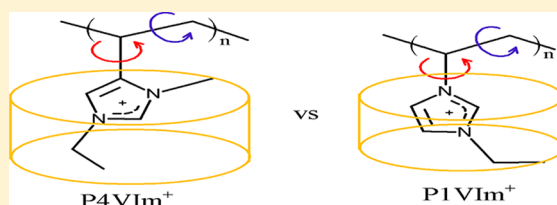
Thomas W. Smith,<sup>\*,†</sup> Meng Zhao,<sup>‡</sup> Fan Yang,<sup>†</sup> Darren Smith,<sup>†</sup> and Peggy Cebe<sup>§</sup>

<sup>†</sup>School of Chemistry & Materials Sciences, College of Science, and <sup>‡</sup>Microsystems Engineering Department, Kate Gleason College of Engineering, Rochester Institute of Technology, Rochester, New York 14623, United States

<sup>§</sup>Physics and Astronomy Department, Center for Nanoscopic Physics, Science and Technology Center, Tufts University, Medford, Massachusetts 02155, United States

## Supporting Information

**ABSTRACT:** The synthesis of 1-ethyl-3-methyl-4-vinylimidazolium triflate, its polymerization, and ion exchange to yield a family of 4-imidazolium polymers with a variety of anions are described. For comparative purposes, the synthesis, polymerization, and ion exchange of an analogous set of 1-vinylimidazolium polymers are also presented. The comparative thermal and dielectric characteristics of the 4-vinyl- and 1-vinylimidazolium salts were evaluated. The trends in the glass transition ( $T_g$ ) characteristics of the various 4-vinylimidazolium and 1-vinylimidazolium polymers were similar; however, the glass transition temperatures of poly(4-vinylimidazolium)  $\text{BF}_4^-$ ,  $\text{PF}_6^-$ ,  $\text{AsF}_6^-$ , and  $\text{CF}_3\text{SO}_3^-$  salts were significantly higher than those of the corresponding poly(1-vinylimidazolium) salts. This difference and the increase in  $T_g$  in going from  $\text{BF}_4^-$  to  $\text{AsF}_6^-$  in the 4-vinylimidazolium series were attributed to enhanced intramolecular bridging between imidazolium moieties positioned 1,3 or 1,5 along the polymer chain. In the dielectric spectra of 1-vinylimidazolium salts at temperatures in excess of 30 °C, one relaxation mode distinct from that for electrode polarization is observed. The single mode appears to correspond to the  $\alpha$ -relaxation peak in poly(3-ethyl-1-vinylimidazolium salts) recently identified and attributed to ion-pair motion by Nakamura et al. In the 4-vinylimidazolium polymer spectra set, at temperatures in excess of 30 °C, two relaxation modes, distinct from that for electrode polarization, are apparent: the  $\alpha$  peak also observed in the 1-vinylimidazolium polymer set and a new relaxation peak observed at lower frequency. The lower frequency relaxation peak is identified in this work as the  $\alpha'$ -relaxation and is also associated with ion-pair motion. Assuming the relaxation processes to be Arrhenius in nature, the activation energy of the  $\alpha$ -relaxation in poly(4-vinylimidazolium)  $\text{BF}_4^-$ ,  $\text{PF}_6^-$ ,  $\text{CF}_3\text{SO}_3^-$ ,  $\text{TFSI}^-$ , and  $\text{C}_2\text{N}_3^-$  salts ranged from 83 to 28 kJ/mol and appears to scale with the glass transition temperature.



## INTRODUCTION AND BACKGROUND

Ionic liquids are salts with low melting points (often below room temperature) and are typically composed of quaternary sulfonium, phosphonium, or ammonium (imidazolium, pyridinium, pyrrolidinium) cations paired with anions of low Lewis basicity ( $\text{BF}_4^-$ ,  $\text{PF}_6^-$ ,  $\text{CF}_3\text{SO}_3^-$  ( $\text{CF}_3\text{SO}_2$ ) $_2\text{N}^-$ , etc.). Today the utility of ionic liquids in electrochemical devices<sup>1</sup> ranging from lithium ion batteries,<sup>2</sup> to fuel cells,<sup>3</sup> capacitors,<sup>4</sup> solar cells,<sup>5</sup> and actuators is being explored. Because of the mobility of both the anionic and cationic components of ionic liquids, the function of some devices might be improved if conventional ionic liquids were replaced by film-forming ionic liquid/polymer gel electrolytes or ionic liquid polymers in which the mobility of one or both the ions is constrained. There are effectively two options for the realization of ionic liquid-based polymer electrolytes: (1) plasticization of a preformed nonionic polymer with an ionic liquid,<sup>6</sup> or polymerization of a nonionic monomer in an ionic liquid to form “ion gels”,<sup>7,8</sup> and (2) synthesis of ionic liquid polyelectrolytes by polymerization of ammonium, sulfonium, or phosphonium monomers,<sup>9</sup> or quaternization of neutral precursor polymers to yield the analogous ammonium, sulfonium, or phosphonium polymers.

The plasticization strategy has been applied in poly(vinylidene fluoride) and vinylidene fluoride/hexafluoropropylene copolymer membranes<sup>10–12</sup> for lithium secondary batteries and fuel cells, transducers,<sup>13</sup> sensors,<sup>14</sup> and electrochromic devices.<sup>15,16</sup>

There are a number of recent reviews<sup>17–21</sup> which document the history and advances in polyionic liquids since the first intentional synthesis by Watanabe et al.<sup>22</sup> of a viscoelastic (rubbery) polymer electrolyte comprising a poly(*N*-butylpyridinium tetrachloroaluminate) eutectic. Regarding the present research, the recent publication by Elabd et al.,<sup>23</sup> which detailed the results of the synthesis and polymerization of (1-[(2-methacryloyloxy)ethyl]-3-butylimidazolium bromide) and its subsequent ion exchange with fluoride-containing anions,  $\text{TFSI}^-$ ,  $\text{BF}_4^-$ ,  $\text{CF}_3\text{SO}_3^-$ , and  $\text{PF}_6^-$ , is particularly relevant. These workers investigated the effect of anion type on the chemical, thermal, and conductive properties of poly(1-[(2-methacryloyloxy)ethyl]-3-butylimidazolium)-based polyionic

Received: April 27, 2012

Revised: December 24, 2012

liquids. The glass transition,  $T_g$ , was found to decrease in the following order:  $\text{Br}^- > \text{PF}_6^- > \text{BF}_4^- > \text{CF}_3\text{SO}_3^- > \text{TFSI}$ . Overall, there was a 95° depression in  $T_g$  from the  $\text{Br}^-$  salt ( $T_g = 102^\circ\text{C}$ ) to the TFSI salt ( $T_g = 7^\circ\text{C}$ ). While the glass transition temperature was found to play a dominant role in determining ion conductivity, other factors, including the size and symmetry of the anion and dissociation energy of the ion pair, were cited as important factors.

The present report also builds on three recent publications by Nakamura et al.<sup>24–26</sup> in which the dielectric relaxation and viscoelastic characteristics of poly(1-vinyl-3-ethylimidazolium trifluoromethylsulfonylimide) (PVIM<sup>+</sup>TFSI<sup>-</sup>) and a family of poly(1-vinyl-3-butylimidazolium salts) were studied.

The dissymmetric, aprotic ionic liquids in this report differ from those previously described in the literature in that they are 1,3-dialkyl-4-vinylimidazolium salts. Figure 1 displays a pentad

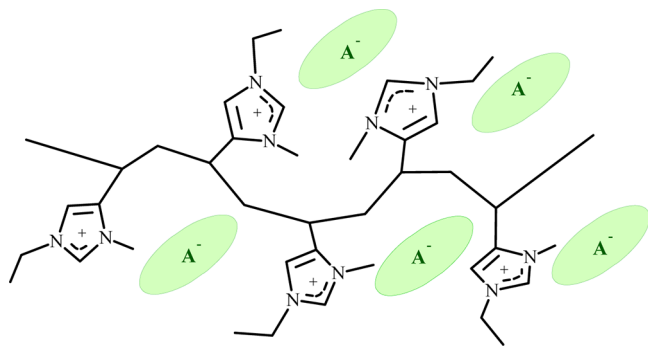


**Figure 1.** Pentad segment of the 1-ethyl-3-methyl-4-vinylimidazolium polymer.

of a poly(1-ethyl-3-methyl-4-vinylimidazolium salt) in which the counterion is sandwiched between pendant functional moieties positioned 1,3 on the polymer backbone. The asymmetric imidazolium moiety is tethered to the polymer backbone at the 4-position of the imidazolium ring.

This tends to result in additional degrees of freedom, increased free volume, and enhanced lateral overlap between proximate imidazole residues that may be situated 1,3 or 1,5 with respect to each other on the carbon chain.

## EXPERIMENTAL SECTION

**Instruments.** *NMR.* Proton NMR spectra were obtained using a Bruker DRX-300 spectrometer. Unless noted, all samples were dissolved in chloroform-*d* (Aldrich, 99.8 atom % D, 0.05% v/v TMS).

*Differential Scanning Calorimetry (DSC).* Glass transition thermograms were obtained under nitrogen using a TA Instruments DSC Q100 equipped with a liquid-nitrogen cooling system. All samples were prepared in an Ar-filled, Vacuum Atmospheres glovebox. Polymer samples were placed in an open, hermetically sealable, aluminum pan and heated to 100 °C for 15 min on the surface of a digital hot plate in the glovebox. The aluminum pan was then capped and sealed. In the DSC, samples were ramped to 200 °C and then cooled to −50 °C at a rate of 20 °C/min. Each sample was held at −50 and 200 °C, respectively, for 1 min in between each heating and cooling cycle.  $T_g$  values are reported as midpoint glass transition temperatures,  $T_g$ -mid. The analysis was a seven-step process: (1) heating from 22 to 200 °C at 20 °C/min; (2) holding for 1 min at 200 °C; (3) cooling from 200 to −50 °C at 20 °C/min; (4) holding for 1 min at −50 °C; (5) heating from −50 to 200 °C at 20 °C/min; (6) holding for 1 min at 200 °C; and (7) cooling from 200 °C to −50 °C at 20 °C/min. It cannot be emphasized too strongly that obtaining accurate, repeatable, measures of the glass transition in poly(ionic liquid) 1-vinyl- and 4-vinylimidazolium salts requires substantial

diligence and care. In the present research, rough correspondence in heating cycle and cooling cycle heat capacity changes were generally required to validate a heat capacity change as a glass transition. Additional validation was garnered by way of a final heating cycle from −50 to 200 °C, heating at 40 °C/min. Under these conditions heating cycle heat capacity changes associated with the glass transition will be amplified and shifted to a somewhat higher temperature.

*Size Exclusion Chromatography.* Molecular weight and polydispersity were determined using an Agilent 1100 series gel permeation chromatograph with two Agilent Zorbax PSM 60-S columns (in series). The samples were eluted at 35 °C, using *N,N'*-dimethylformamide as the solvent. Molecular weight values reported are styrene equivalent molecular weights based on hydrodynamic radius.

*Dielectric Spectroscopy.* Dielectric properties were measured with an ARES rheometer system from TA Instruments coupled with an Agilent LCR Meter 4284A. Polymer films whose thickness ranged from 250 to 1600 μm were prepared by solution casting from ethanol or DMF on Al foil substrates at ambient temperature. The films were dried in a fume hood at room temperature and cut to 22 mm by 24 mm before a final drying process in which they were further dried at 120 °C on the surface of a digital hot plate for at least 24 h. The dried films were then stored in a desiccator until use. The samples were placed between two stainless steel electrodes in the ARES and isothermally measured as a function of frequency, between 20 and 10<sup>6</sup> Hz. The temperature was controlled by the ARES with liquid nitrogen and compressed air as the gas at low and high temperatures, respectively.

The Havriliak–Negami (HN) model<sup>27</sup> is used to analyze the dielectric relaxation measurements. The complex dielectric function,  $\epsilon^*(\omega) = \epsilon' - i\epsilon''$ , is written as

$$\epsilon^*(\omega) = \epsilon_\infty + \frac{\Delta\epsilon}{(1 + (i\omega\tau)^\beta)^\gamma} - i\frac{\sigma_0}{\omega^s\epsilon_0} \quad (1)$$

where  $\omega = 2\pi f$  is the radian electric field oscillation frequency,  $\epsilon_\infty$  is the high-frequency limit of the dielectric constant,  $\Delta\epsilon$  is the relaxation strength, defined as  $\Delta\epsilon = \epsilon_s - \epsilon_\infty$ , and  $\tau$  is the relaxation time which is the reciprocal of the radian frequency of maximal loss,  $\omega_{\max}$ .  $\beta$  and  $\gamma$  ( $0 < \beta \leq 1$ ,  $0 < \beta\gamma \leq 1$ ) are the shape parameters of the relaxation spectra. For a purely Debye relaxation process, both  $\beta$  and  $\gamma$  would be equal to unity. The added term,  $-i(\sigma_0/\epsilon_0\omega^s)$ , refers to effects of conduction, where  $\sigma_0$  is related to dc conductivity and  $\epsilon_0$  is the permittivity of vacuum. The exponential parameter,  $s$ , is equal to 1 for ohmic conductivity and less than 1 for nonohmic effects in the conductivity.<sup>28</sup> The relationship between frequency at maximum loss,  $f_{\max}$ , which is known as the relaxation rate, and the corresponding temperature can be described by an Arrhenius function. The frequency of maximum loss,  $f_{\max}$ , was most often evaluated directly from plots of  $\tan \delta (= \epsilon''/\epsilon')$  vs frequency. In three instances [poly(1-ethyl-3-methyl-4-vinylimidazolium PF<sub>6</sub><sup>-</sup>), poly(3-ethyl-1-vinylimidazolium PF<sub>6</sub><sup>-</sup>), and poly(1-ethyl-3-methyl-4-vinylimidazolium BF<sub>4</sub><sup>-</sup>)] additional data were obtained by fitting plots of  $\epsilon''$  vs frequency, according to eq 1, with  $\Delta\epsilon$ ,  $\tau$ ,  $\beta$ ,  $\gamma$ ,  $\sigma_0$ , and  $s$  as fitting parameters.

**Materials.** *Reagent Chemicals.* Unless otherwise noted, all reagent chemicals were used as received without further purification. 1,1,1,3,3,3-Hexamethyldisilazane (99.9%), 1-vinylimidazole (99+%), 2,2'-azobisisobutyronitrile (AIBN, 98%, recrystallized from methanol), 4-imidazoleacrylic acid (99%), calcium hydride (coarse granules, 0–20 mm, 95%), ethyl trifluoromethanesulfonate (99%), lithium hexafluorophosphate (LiPF<sub>6</sub>, 98%), lithium trifluoromethanesulfonylimide (LiTFSI, 99.95%), picric acid (99+%), and tetrafluoroboric acid (48 wt % solution in water) were purchased from Sigma-Aldrich. 4-*tert*-Butyl catechol (4-TBC, 99%), ammonium sulfate (reagent ACS), iodomethane (stabilized, 99%), isopropanol (IPA, analysis), methyl alcohol (reagent ACS, 99.8%), potassium carbonate (reagent grade ACS, anhydrous), sodium bicarbonate (p.a.), and sodium dicyanamide (97% pure) were purchased from Acros Organic. Ethyl acetate (EA, AR ACS), hydrochloric acid (AR ACS), and dichloromethane (AR ACS) were obtained from Mallinckrodt Chemicals. Magnesium sulfate

(anhydrous powder) was obtained from J.T. Baker, *N,N*-Dimethylformamide (Spectrograde), benzene (GR ACS), acetonitrile (GR ACS), and hexanes (GR ACS) were obtained from EMD.

**4(5)-Vinylimidazole.** 4(5)-Vinylimidazole was synthesized by a procedure analogous to that of Overberger et al.<sup>29</sup> by means of the decarboxylation of urocanic acid. In a typical procedure, urocanic acid (5.00 g, 36.2 mmol) was decarboxylated in a 100 mL single-neck round-bottom flask with attached elbow. This flask was heated in an oil bath at 230 °C under vacuum (10  $\mu$ mHg), and crude 4(5)-vinylimidazole was collected, as a pale yellow viscous liquid, over a period of about 3 h. The 4(5)-vinylimidazole was then cooled overnight at 10 °C to obtain a yellow crystalline material. Yield = 2.03 g, 60%.

**1-Trimethylsilyl-4-vinylimidazole.** The synthesis of 1-trimethylsilyl-4-vinylimidazole was carried out in a procedure analogous to that of Kawakami and Overberger.<sup>30</sup> Thus, crude 4(5)-vinylimidazole (5.00 g, 53.1 mmol), 1,1,1,3,3,3-hexamethyldisilazane (8.57 g, 53.1 mmol), benzene (20 mL, 225 mmol), ammonium sulfate (catalytic amount), and 4-*tert*-butyl catechol (catalytic amount) were charged to a 50 mL three-neck round-bottom flask. The three-neck flask was equipped with a Teflon adapter with thermometer, 14/20 ground-glass stopper, reflux condenser with gas inlet valve, and a magnetic stir bar. The reaction mixture was blanketed with argon, heated, and stirred in an oil bath at 95 °C for 20 h. The reaction mixture was then allowed to come to room temperature, and the solvent was removed by rotary evaporation. The remaining clear oil was purified by vacuum distillation. The resulting oil crystallized when stored at 10 °C. Yield = 7.47 g, 85%; bp = 50 °C, 0.13 mmHg.

**1-Methyl-5-vinylimidazole.** The synthesis of 1-methyl-5-vinylimidazole was carried out by a procedure analogous to that of Kawakami and Overberger.<sup>30</sup> Thus, pure 1-trimethylsilyl-4-vinylimidazole (7.47 g, 44.9 mmol) was reacted with iodomethane (6.06 g, 42.7 mmol) to give 1-trimethylsilyl-3-methyl-4-vinylimidazolium iodide, which was hydrolyzed to give 1-methyl-5-vinylimidazole; crude yield = 2.52 g, 64%. Picric acid was added, and the crude product was stored at 10 °C until purified by distillation.

**1-Ethyl-3-methyl-4-vinylimidazolium Triflate.** Freshly distilled 1-methyl-5-vinylimidazole (4.22 g, 39.1 mmol) and dichloromethane (50 mL) were charged to a 250 mL three-neck round-bottom flask, equipped with gas inlet valve, Teflon adapter with thermometer, addition funnel, and magnetic stir bar. The solution was cooled to 0 °C by immersion in an ice–water bath and stirred under an argon blanket. Ethyl trifluoromethanesulfonate, [6.1 mL (8.37 g), 47 mmol] and dichloromethane (50 mL) were added to the addition funnel, and this solution was added dropwise over a 30 min period. The reaction mixture was held at 0 °C and stirred for 2 h. The addition funnel was replaced by a short-path distillation head, and the solvent was removed *in vacuo*, yielding 10.64 g, 95%, of 3-ethyl-1-methyl-5-vinylimidazolium triflate as a white crystalline solid; mp = 41 °C. The reaction vessel was immersed in a 0 °C ice/water bath throughout this process. <sup>1</sup>H NMR (in THF-*d*<sub>6</sub>) 1.47 (3H, t, N–CH<sub>2</sub>CH<sub>3</sub>), 3.81 (3H, s, N–CH<sub>3</sub>), 4.18 (2H, q, N–CH<sub>2</sub>CH<sub>3</sub>), 5.54 (1H, d, <sup>3</sup>J 11.31 Hz, *cis*-vinyl H), 5.88 (1H, d, <sup>3</sup>J 17.46 Hz, *trans*-vinyl H), 6.54 (1H, <sup>3</sup>J<sub>*cis*</sub> 11.31, <sup>3</sup>J<sub>*trans*</sub> 17.46, vinyl H–C), 7.75 (1H, s, C-4H), 8.92 (1H, s, C-2H). The alkylation reaction can be carried out at 0 °C in ethyl acetate. The reaction in ethyl acetate is slower, and one should allow for 6 h to drive the reaction to completion. Reaction in ethyl acetate enables one to proceed directly to polymerization without the need for solvent removal.

**Poly(1-ethyl-3-methyl-4-vinylimidazolium triflate) (P4VIm<sup>+</sup>CF<sub>3</sub>SO<sub>3</sub><sup>−</sup>).** 1-Ethyl-3-methyl-4-vinylimidazolium triflate (5.3 g, 39 mmol) was dissolved in ethyl acetate (30 mL) and transferred to a polymerization tube at 0 °C, under an argon blanket. A solution was made of AIBN (0.03 g, 0.183 mmol) by dissolution in ethyl acetate (10 mL). The AIBN solution (1 mL) was added to the polymerization tube and mixed. The solution was then degassed by three freeze–thaw cycles by freezing the contents in liquid nitrogen (−192 °C). The tube was then flame-sealed and immersed in a water bath at 65 °C for 20 h. The resulting polymer gel was isolated by dissolution in methanol and precipitation in methyl *tert*-butyl ether. The precipitate was dried on a

hot plate at 90 °C for 1 h in an Ar-filled, Vacuum Atmospheres glovebox. Yield = 3.07 g, 88%, *M*<sub>n</sub> = 8730 g/mol, *M*<sub>w</sub> = 14 722 g/mol, PD = 1.7.

**3-Ethyl-1-vinylimidazolium Triflate.** 3-Ethyl-1-vinylimidazolium triflate was synthesized in a reaction analogous to that for the synthesis of 1-ethyl-3-methyl-4-vinylimidazolium triflate. Thus, freshly distilled 1-vinylimidazole (1.73 g, 18.4 mmol) was charged to a 250 mL three-neck round-bottom flask, equipped with gas inlet valve, Teflon adapter with thermometer, addition funnel, and magnetic stir bar. The solution was cooled to 0 °C by immersion in an ice–water bath and stirred under an argon blanket. Ethyl trifluoromethanesulfonate (3.93 g, 22.1 mmol, 1.2 equiv) and dichloromethane (50 mL) were added to the addition funnel, and this solution was added dropwise over a 30 min period. The reaction mixture was held at 0 °C and stirred for 1.5 h. The addition funnel was replaced by a short-path distillation head, and the solvent was removed *in vacuo*, yielding 5 g, 99%, of 3-ethyl-1-vinylimidazolium triflate.

**Poly(3-ethyl-1-vinylimidazolium triflate) (P1VIm<sup>+</sup>CF<sub>3</sub>SO<sub>3</sub><sup>−</sup>).** P1VIm<sup>+</sup>CF<sub>3</sub>SO<sub>3</sub><sup>−</sup> was polymerized and isolated by a process analogous to that employed in the synthesis of P4VIm<sup>+</sup>CF<sub>3</sub>SO<sub>3</sub><sup>−</sup>. Yield = 4.90 g, 99%, *M*<sub>n</sub> = 15 706 g/mol, *M*<sub>w</sub> = 18 968 g/mol, PD = 1.21.

**Ion Exchange.** The ion-exchange process employed with 4-vinyl- and 1-vinylimidazolium triflate polymers was the same. In a typical procedure, 5 mL of a methanol solution containing 1.84 mmol of imidazolium triflate polymer was added to a centrifuge tube, to which a 4 M excess of a methanol or methanol/water solution of a TFSI, dicyanamide, hexafluorophosphate, or hexafluoroarsenate salt was added. The solution was shaken vigorously, and a precipitate formed. The precipitate was isolated by centrifugation, decanted, and subjected to at least three methanol wash/centrifugation cycles prior to drying under Ar in a Vacuum Atmospheres glovebox, < 1 ppm H<sub>2</sub>O. The tetrafluoroborate salt was prepared by a similar procedure mixing 5 mL of a methanol solution containing 1.84 mmol of imidazolium triflate polymer with 5 mL of water containing 79.5 mmol of tetrafluoroboric acid.

## RESULTS AND DISCUSSION

The present effort to prepare 4(5)-vinylimidazolium polymers was initially motivated by the idea that, as compared to 1-vinylimidazolium polymers, attachment at the 4(5)-position of the imidazole ring would afford increased rotational and translational freedom for the imidazolium moiety. Moreover, increased degrees of freedom and greater asymmetry may allow for greater free volume and greater ability for the imidazolium moiety to interact cooperatively in the transport of target ions. The cylindrical volume required by a rotating imidazolium group tethered to the polymer backbone at the 4 and 1 positions of the imidazolium ring and the bonds around which rotation is possible are depicted in Figure 2.

The focus of this paper is the 4-vinylimidazolium homopolymer and understanding how its glass transition and dielectric properties, as compared to 1-vinylimidazolium homopolymers, change with variation of the counterion. Accordingly, the synthesis of 1-ethyl-3-methyl-4-vinylimidazo-

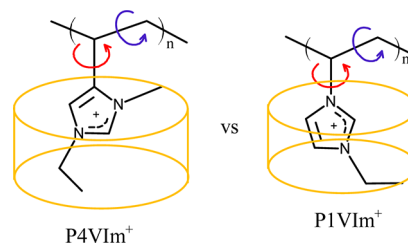


**Figure 2.** Asymmetry and rotational degrees of freedom in P4VIm<sup>+</sup> and P1VIm<sup>+</sup>.

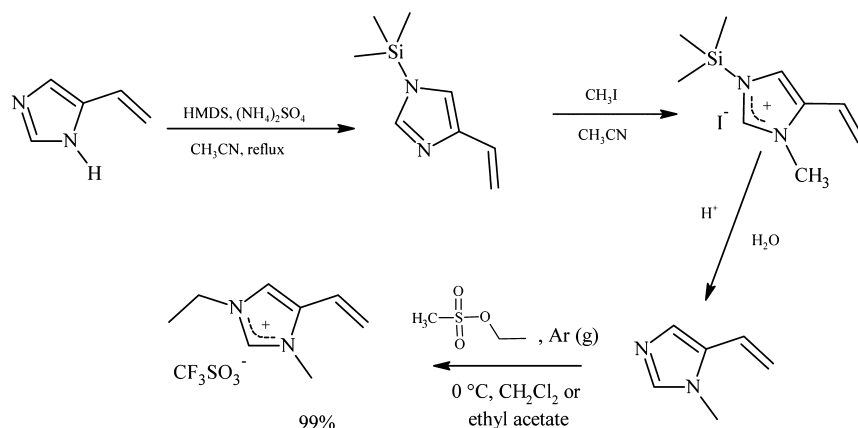


Figure 3. Synthesis of 1-ethyl-3-methyl-4-vinylimidazolium triflate.

lium triflate, its polymerization, and ion exchange to yield a family of 4-imidazolium polymers with a variety of anions are described. The glass transition, thermal stability, and dielectric relaxation characteristics of these related polymers are also reported and discussed. For comparative purposes, the synthesis, polymerization, ion exchange, and thermal and dielectric characteristics of an analogous set of 1-vinylimidazolium polymers are also presented. The goal is to better understand how the relative degree of freedom of the imidazolium moiety tethered to the polymer backbone and the size and character of the counterion influence the glass transition and molecular relaxations in these “polyionic liquids”.

**Synthesis, Polymerization, and Ion Exchange of 4-Vinyl- and 1-Vinylimidazolium Monomers.** The synthesis of a quaternary 4-vinylimidazolium monomer was first reported in 2004 by Wang and Smith.<sup>31</sup> In that preliminary work, 1-butyl-3-methyl-4-vinylimidazolium iodide was simply prepared by alkylation of 1-methyl-5-vinylimidazole with butyl iodide. However, the iodide anion interfered with its free-radical polymerization. The aqueous solution of the iodide monomer was ion-exchanged with  $\text{LiPF}_6$  to yield an ionic liquid monomer,  $T_g = -12$  °C. The  $\text{PF}_6^-$  monomer tends to polymerize spontaneously as it oils out of the aqueous solution. However, the exploratory work served both to confirm that an ionic liquid 1-alkyl-3-methyl-4-vinylimidazolium salt can be synthesized and to elucidate the fact that, as was the case with 4-vinylpyridinium salts,<sup>32</sup> the key problem that must be overcome was to suppress its spontaneous polymerization.

The work of Fife et al.<sup>33</sup> in synthesizing 4-vinylpyridinium salts teaches that isolable, storage stable, 4- and 5-vinyl-1-methyl-3-alkylimidazolium salts might be synthesized if the alkylation is carried out under anhydrous conditions with triflate esters. This has proven to be the case. Thus, 1-ethyl-3-methyl-4-vinylimidazolium triflate was quantitatively synthesized, as depicted in Figure 3, from 4(5)-vinylimidazole. 1-Methyl-5-vinylimidazole was purified by vacuum distillation prior to direct alkylation with ethyl triflate, at 0 °C, in methylene chloride or ethyl acetate. The crystalline, ionic liquid monomer, mp = 41 °C, was obtained, in a pure dry (water-free) state, by removal of solvent *in vacuo* at 0 °C.

The preparations of 1-vinylimidazolium salts, which have been described in the literature,<sup>34–37</sup> do not present the synthetic challenges inherent in the synthesis of the 1,3-dialkyl-4-vinylimidazolium analogues in that they do not spontaneously polymerize at ambient temperatures. Indeed, the various ionic liquid 1-vinylimidazolium monomer salts can be

prepared by ion exchange of aqueous solutions of their halide salts. Nevertheless, in order to obtain the 1-vinylimidazolium monomer in a pure and dry state, the process of direct alkylation with ethyl triflate, which was used to prepare our 4-vinylimidazolium triflate, was also used to synthesize 3-ethyl-1-vinylimidazolium triflate.

1-ethyl-3-methyl-4-vinylimidazolium triflate and 3-ethyl-1-vinylimidazolium triflate were homopolymerized free-radically in ethyl acetate, initiating with AIBN. The triflate polymers that precipitate from ethyl acetate were dissolved in methanol and purified by precipitation in ether. Molecular weights were evaluated by GPC. Details are presented in the Experimental Section.

The various poly(1-ethyl-3-methyl-4-vinylimidazolium) and poly(3-ethyl-1-vinylimidazolium) salts were obtained by simply ion-exchanging methanolic solutions of the 4-vinyl- or 1-vinylimidazolium triflate polymers with methanol or water solutions of protic or alkali metal salts of the desired anion. The water or methanol insoluble  $(\text{CF}_3\text{SO}_3)_2\text{N}^-$ ,  $\text{C}_2\text{N}_3^-$ ,  $\text{BF}_4^-$ ,  $\text{PF}_6^-$ , and  $\text{AsF}_6^-$  ion-exchanged polymers precipitated and were isolated and purified, as described in the Experimental Section, by centrifugation and washing. The anions that were employed differ in geometry and polarizability. The triflate salt is a classic semispherical “hard anion” in which the electrons surrounding the sulfonate group are not highly polarizable. Trifluoromethylsulfonamide is a bent, tetrahedral, plasticizing anion in which the anionic charge on the nitrogen atom is soft and polarizable. Dicyanamide is a less solvating, bent, tetrahedral, anion in which the anionic charge is soft polarizable and delocalized over an ambident anion. Tetrafluoroborate, hexafluorophosphate, and hexafluoroarsenate are a family non-nucleophilic complex anions derived from Lewis acids in which the volume of the anion increases from 0.073 to 0.109 to 0.121 nm<sup>3</sup>, respectively.<sup>38</sup>

**The Glass Transition.** It is often said that the glass transition in polymeric liquids is a poorly understood phenomenon. This is particularly true for ionic polymers whose glass transition characteristics have received only limited attention since the early analysis by Eisenberg et al.<sup>39</sup> in which the glass transitions of ionic polymers were found to be proportional to the ratio of the counterion charge,  $q$ , to the distance between the centers of cations and anions,  $a$ . Following on the work of Eisenberg, Tsutsui and Tanaka<sup>40</sup> reported that the glass transition temperatures of ionic polymers could be correlated with cohesive energy density

$$\text{CED}_{\text{ionic}} = N_{\text{A}} e^2 \left( \frac{\rho q_{\text{c}}}{M a} \right) \quad (2)$$

in accordance with eq 2

$$T_{\text{g}} = K_1 \left( N_{\text{A}} e^2 \left( \frac{\rho q_{\text{c}}}{M a} \right) \right)^n \quad (3)$$

where  $N_{\text{A}}$  is Avogadro's number,  $e$  is the electronic charge,  $\rho$  is the polymer density,  $M$  is the molecular weight per skeletal ion, and  $a$  is the equilibrium distance between the center of the anion and the cation. Equation 3 shows that the glass transition temperature is directly proportional to the cohesive energy density multiplied by a coefficient,  $K_1$ . The coefficient varies from polymer to polymer, and in keeping with the analysis by Eisenberg, the glass transition temperature is predicted to be inversely proportional to the distance between the anion and the cation.

Agapov has studied the effect of polar interactions on the temperature dependence of structural (segmental) and chain dynamics in polymeric liquids.<sup>41</sup> The glass transition temperature,  $T_{\text{g}}$ , and fragility index,  $m$ , were found to depend on the monomer's polarity and the relative position of the polar group. The effect of polar interactions on  $T_{\text{g}}$  and  $m$  is discussed in terms of a balance between changes in the cohesive energy and conformational rigidity.

In the present research, the glass transition in 4-vinyl- and 1-vinylimidazolium polymers was evaluated by differential scanning calorimetry (DSC). The results of a comparative DSC analysis of the glass transition temperature of the full set of ion-exchanged 4-vinylimidazolium polymers and 1-vinylimidazolium polymers are presented in Table 1. Heating cycle

**Table 1. Glass Transition Temperatures of Poly(imidazolium salts)**

anion	P4VIm <sup>+</sup> salts		P1VIm <sup>+</sup> salts	
	heating cycle	cooling cycle	heating cycle	cooling cycle
	$T_{\text{g-mid}}$ (°C)	$T_{\text{g-mid}}$ (°C)	$T_{\text{g-mid}}$ (°C)	$T_{\text{g-mid}}$ (°C)
BF <sub>4</sub> <sup>-</sup>	186	178	106	97
PF <sub>6</sub> <sup>-</sup>	200	180	141	113
AsF <sub>6</sub> <sup>-</sup>	213	208	122	
CF <sub>3</sub> SO <sub>3</sub> <sup>-</sup>	153	140	140	124
(CF <sub>3</sub> SO <sub>2</sub> ) <sub>2</sub> N <sup>-</sup>	88	63	97	74
C <sub>2</sub> N <sub>3</sub> <sup>-</sup>	89	103	105	95

and cooling cycle glass transition values are tabulated. Cooling cycle  $T_{\text{g-mid}}$  values are somewhat lower than the heating cycle  $T_{\text{g-mid}}$  values. This may be a result of a longer time constant for the reformation of the glass, which results in a heat capacity change over broader temperature range in the cooling cycle.<sup>42</sup> Figure 4 displays the second heating cycle and subsequent cooling cycle in the DSC thermogram for P4VIm<sup>+</sup>TFSI<sup>-</sup>. The thermogram is typical of those observed across the series of poly(4-vinylimidazolium salts).<sup>43</sup>

The consistency of heating cycle and cooling cycle data provides significant support for the validity of the  $T_{\text{g}}$  values presented. Tetrafluoroborate, BF<sub>4</sub><sup>-</sup>, hexafluorophosphate, PF<sub>6</sub><sup>-</sup>, and hexafluoroarsenate, AsF<sub>6</sub><sup>-</sup>, comprise a set of complex fluoride anions of increasing size. In the 1-ethyl-3-methyl-4-vinylimidazolium polymer set, the heating cycle  $T_{\text{g-mid}}$  increased from 186 °C to 200 °C and 213 °C when the triflate polymer was ion-exchanged to BF<sub>4</sub><sup>-</sup>, PF<sub>6</sub><sup>-</sup>, and AsF<sub>6</sub><sup>-</sup>,

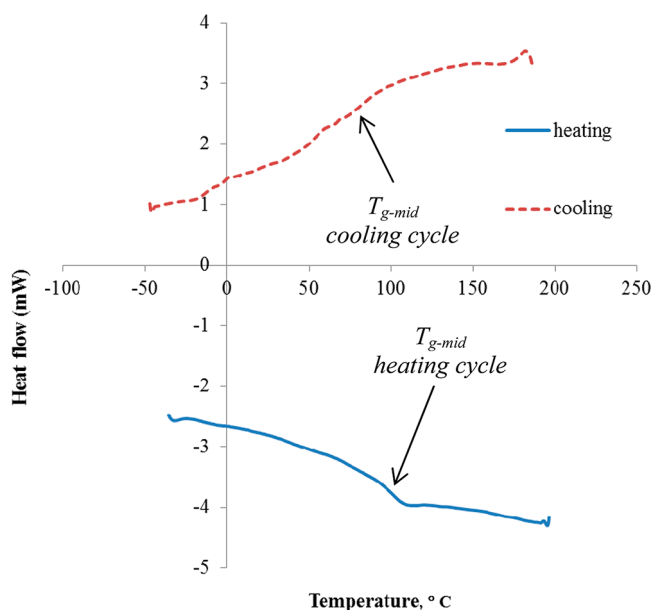


**Figure 4.** DSC scans of P4VIm<sup>+</sup>TFSI<sup>-</sup> during heating and subsequent cooling.

respectively. This result cannot be rationalized on the basis of the change in the ratio of the counterion charge,  $q$ , to the distance between the centers of cations and anions,  $a$ . Enhanced intersegmental and intramolecular interactions (bridging between imidazolium ions by the anion) may be a dominant factor in driving the  $T_{\text{g}}$  increase in this series. The 4-vinylimidazolium polymers with TFSI<sup>-</sup> and C<sub>2</sub>N<sub>3</sub><sup>-</sup> anions exhibit the lowest glass transition temperatures. The lower glass transition temperatures of these two polymers may be a result of plasticization by large solvating anions, which, because of their soft nucleophilic character, allows for association between anion and cation over a larger distance.

As a complement to our studies of poly(1-ethyl-3-methyl-4-vinylimidazolium salts), the glass transition characteristics of corresponding poly(1-vinylimidazolium salts) were analyzed. Table 1 also displays the heating cycle and cooling cycle  $T_{\text{g-mid}}$  values for the family of 3-ethyl-1-vinylimidazolium salts. Heat capacity changes in the cooling cycle, consistent with the heating cycle glass transition temperatures, were observed in the BF<sub>4</sub><sup>-</sup>, PF<sub>6</sub><sup>-</sup>, CF<sub>3</sub>SO<sub>3</sub><sup>-</sup>, TFSI, and C<sub>2</sub>N<sub>3</sub><sup>-</sup>. In the AsF<sub>6</sub><sup>-</sup> salt of the 3-ethyl-1-vinylimidazolium polymer, a heat capacity change that can be attributed to the glass transition was not observed in the cooling cycle.

The first difference of note between the glass transition characteristics of the 1-vinyl- and 4-vinylimidazolium polymers is that, in spite of the greater free volume required for the 1-ethyl-3-methyl-4-vinylimidazolium moiety, the glass transition temperatures of the 4-vinylimidazolium BF<sub>4</sub><sup>-</sup>, PF<sub>6</sub><sup>-</sup>, AsF<sub>6</sub><sup>-</sup>, and CF<sub>3</sub>SO<sub>3</sub><sup>-</sup> salts are higher than those of the corresponding 1-vinylimidazolium salts. Another difference of note is that, in the 1-vinylimidazolium polymer set, the glass transition of the BF<sub>4</sub><sup>-</sup>, PF<sub>6</sub><sup>-</sup>, and AsF<sub>6</sub><sup>-</sup> series does not increase monotonically with increase of anion size. Instead, while the glass transition in this series of non-nucleophilic complex fluoride anions increases significantly in going from the BF<sub>4</sub><sup>-</sup> salt to the PF<sub>6</sub><sup>-</sup> salt, the  $T_{\text{g}}$  of the AsF<sub>6</sub><sup>-</sup> salt is dramatically lower than that of the PF<sub>6</sub><sup>-</sup> salt.

The glass transition temperatures of the TFSI<sup>-</sup> and dicyanamide derivatives of the 1-vinylimidazolium polymer

are slightly higher than those for the corresponding 4-vinylimidazolium salts. As with the TFSI<sup>-</sup> and C<sub>2</sub>N<sub>3</sub><sup>-</sup> salts of the 4-vinylimidazolium polymers, the 1-vinylimidazolium salts with plasticizing TFSI<sup>-</sup> and C<sub>2</sub>N<sub>3</sub><sup>-</sup> anions exhibit the lowest glass transition temperatures.

**Thermal Gravimetric Analysis of Imidazolium Polymers.** The comparative thermal gravimetric analysis (TGA) of the triflate polymers, presented in Figure 5, shows that the 4-

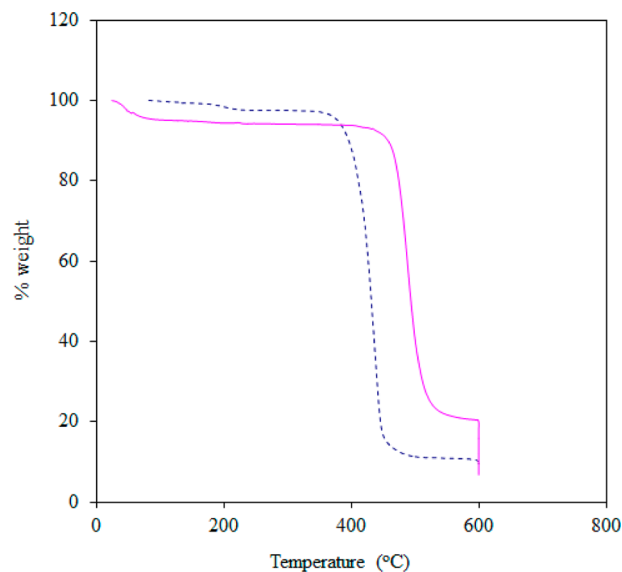


**Figure 5.** TGA of P1VIm<sup>+</sup>CF<sub>3</sub>SO<sub>3</sub><sup>-</sup> [dashed blue line], and P4VIm<sup>+</sup>CF<sub>3</sub>SO<sub>3</sub><sup>-</sup> [solid violet line].

vinyl imidazolium polymer has greater thermal stability than the 1-vinylimidazolium polymer. The TGA results that were obtained in the present research for poly(3-ethyl-1-vinylimidazolium triflate), P1VIm<sup>+</sup>CF<sub>3</sub>SO<sub>3</sub><sup>-</sup>, correspond well with those published by Marcilla et al.<sup>35</sup> Under nitrogen, P1VIm<sup>+</sup>CF<sub>3</sub>SO<sub>3</sub><sup>-</sup> suffers extensive mass loss at 400 to 448 °C. Significant mass loss in poly(1-ethyl-3-methyl-4-vinylimidazolium triflate), P4VIm<sup>+</sup>CF<sub>3</sub>SO<sub>3</sub><sup>-</sup>, occurs in the 467–527 °C temperature range. The increased thermal stability is apparently due to the difference in the tethering point of the imidazolium ring to the polymer backbone. The energy required to break the carbon–carbon bond is some 40 kJ/mol<sup>44</sup> greater than that required to break a carbon–nitrogen single bond. The modest reduction in mass below 400 °C is due to loss of absorbed moisture.

**Dielectric Studies.** Dielectric spectroscopy provides simultaneous measurements of dc conductivity and relaxation processes as a function of temperature. Nakamura et al.<sup>24</sup> have reported on the dielectric relaxation characteristics P1VIm<sup>+</sup>TFSI<sup>-</sup> in the frequency range of 10 mHz to 2 MHz and the temperature range of –90 to 90 °C. Three relaxation modes were observed and identified as β, α, and EP (electrode polarization). The β relaxation mode, which is observed at low temperature (–90 to 0 °C), was attributed to the rotational relaxation mode of the imidazolium moiety. Expected dielectric relaxation peaks related to an ion-pair relaxation mode and rotational relaxation motion of TFSI<sup>-</sup> in the bulk polymer were not observed.<sup>24</sup> More recently, using dynamic viscoelastic measurements, Nakamura<sup>25</sup> investigated the same material. Upon comparison of the viscoelastic master curves and the dielectric relaxation spectra, they concluded that the slow

dielectric relaxation mode (the α-relaxation in P1VIm<sup>+</sup>TFSI<sup>-</sup>) was associated with ion-pair motion and not with segmental motion of the imidazolium polymer chain.<sup>25</sup>

In the present research, the dielectric relaxation behavior of a series of ionic liquid polymers [P4VIm<sup>+</sup>CF<sub>3</sub>SO<sub>3</sub><sup>-</sup>, TFSI<sup>-</sup>, C<sub>2</sub>N<sub>3</sub><sup>-</sup>, BF<sub>4</sub><sup>-</sup>, PF<sub>6</sub><sup>-</sup>, and AsF<sub>6</sub><sup>-</sup>] derived from 1-ethyl-3-methyl-4-vinylimidazolium triflate and [P1VIm<sup>+</sup>TFSI<sup>-</sup>, C<sub>2</sub>N<sub>3</sub><sup>-</sup>, and PF<sub>6</sub><sup>-</sup>] derived from 1-ethyl-3-vinylimidazolium triflate was evaluated in the frequency range of 20 Hz to 1 MHz and the temperature range of 30–210 °C. Dipolar relaxations were analyzed by fitting the dielectric loss ε'' using the Havriliak–Negami model, in eq 1. Figure 6 shows experimental ε'' vs frequency data, the deconvoluted α-relaxation peak, and the fit to the Havriliak–Negami equation for P4VIm<sup>+</sup>PF<sub>6</sub><sup>-</sup> at 130 °C.

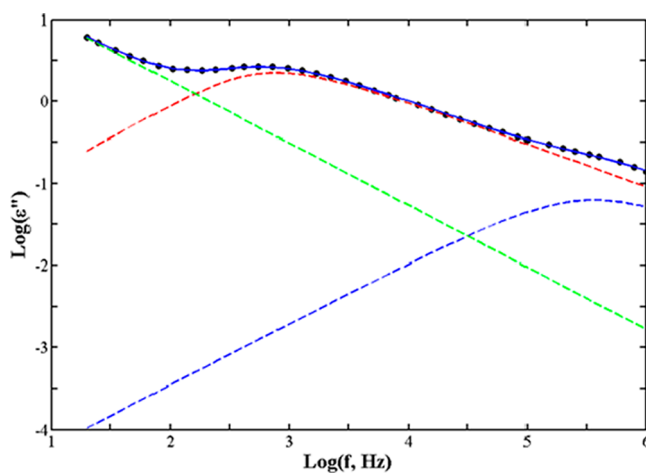


**Figure 6.** ε'' vs frequency for poly(1-ethyl-3-methyl-4-vinylimidazolium PF<sub>6</sub><sup>-</sup>) at 130 °C. Points refer to measured data. Solid blue curve is the summation of individual fitted curves for the α'- and α-relaxations and dc conductivity reflecting the best fit to the data. Dashed red curve: deconvoluted α'-relaxation peak ( $\Delta\epsilon = 6.4$ ,  $\tau = 1.9 \times 10^{-3}$  s,  $\beta = 0.83$ ,  $\gamma = 0.6$ ); dashed blue curve: deconvoluted α-relaxation peak ( $\Delta\epsilon = 0.18$ ,  $\tau = 3.0 \times 10^{-6}$  s,  $\beta = 0.74$ ,  $\gamma = 0.86$ ); dashed green line: dc conductivity ( $\sigma = 2.1 \times 10^{-9}$  S/cm;  $s = 0.76$ ).

Figure 7a–f displays dielectric spectra (ε', ε'', and tan δ versus frequency at 30–210 °C) for P4VIm<sup>+</sup>PF<sub>6</sub><sup>-</sup> and P1VIm<sup>+</sup>PF<sub>6</sub><sup>-</sup>. Below 150 °C, the dielectric constant, ε', in these two polymers is of the order of 70 and is substantially invariant with frequency. Above 110 °C, the dielectric constant increases dramatically at frequencies below 10<sup>5</sup> Hz and is indicative of one or more relaxation processes. These relaxation processes are apparent in both the ε'' and tan δ spectra; however, relaxation peaks are most clearly resolved in the tan δ spectra. In the ε'' and tan δ spectra of P1VIm<sup>+</sup>PF<sub>6</sub><sup>-</sup> (Figure 7c,e) one relaxation mode distinct from that for electrode polarization is observed in the temperature range 30–130 °C. This relaxation appears well below the DSC glass transition; accordingly, it is clearly not associated with segmental motion. The single peak in the dielectric spectra of the P1VIm<sup>+</sup>PF<sub>6</sub><sup>-</sup> set may correspond to the relaxation that Nakamura assigned as the α-relaxation<sup>24</sup> in P1VIm<sup>+</sup>TFSI<sup>-</sup> and attributed to ion-pair motion.<sup>25</sup>

In the P4VIm<sup>+</sup>PF<sub>6</sub><sup>-</sup> spectra set (Figure 7d,f) two relaxation modes, distinct from that for electrode polarization, are apparent, the α-relaxation (observed in the 30–150 °C temperature range) and a new relaxation peak (observed at lower frequency in the 130–210 °C temperature range) that is

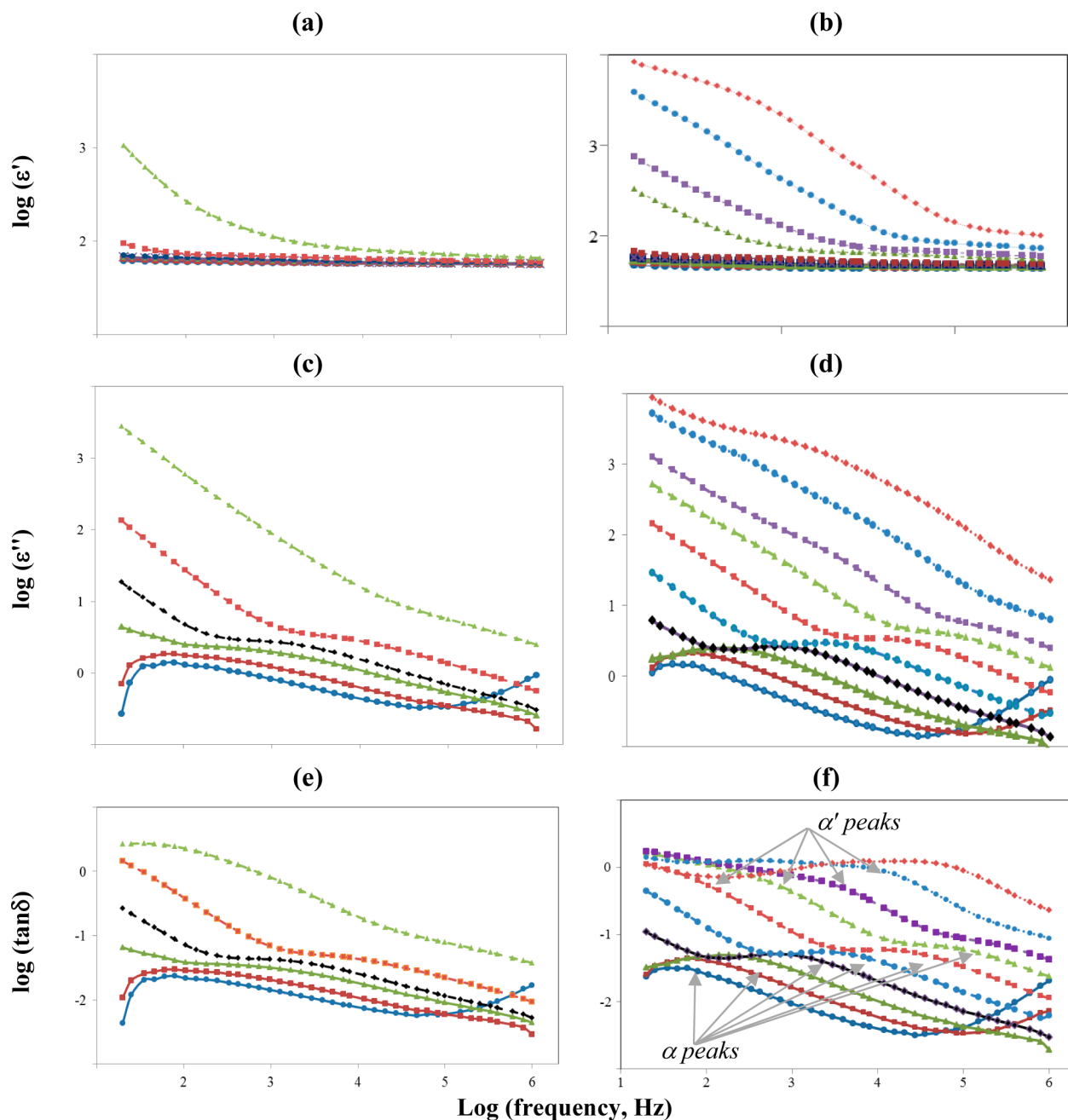


**Figure 7.** (a–f) Frequency dependence of dielectric characteristics,  $\epsilon'$ ,  $\epsilon''$ , and  $\tan \delta$  of P1VIm<sup>+</sup>PF<sub>6</sub><sup>-</sup> (a, c, e) and P4VIm<sup>+</sup>PF<sub>6</sub><sup>-</sup> (b, d, f). Data points of different shape and color connected by solid or dashed lines of the same color are measured data at different temperatures: ● blue solid, 30 °C; ■ red solid, 50 °C; ▲ green solid, 70 °C; ◆ black solid, 90 °C; ● blue dashed, 110 °C; ■ red dashed, 130 °C; ▲ green dashed, 150 °C; ■ purple dashed, 170 °C; ● blue dotted, 190 °C; ◆ orange dotted, 210 °C.

labeled as  $\alpha'$ . Nakamura<sup>24–26</sup> has clearly shown that there are additional  $\beta$ -relaxation modes in the lower temperature regime. In our work, the temperature range examined was 30–230 °C, and the lower temperature  $\beta$ -relaxation modes were not accessible.

The  $\alpha'$ -relaxation is revealed in P4VIm<sup>+</sup>PF<sub>6</sub><sup>-</sup> (but not in P1VIm<sup>+</sup>PF<sub>6</sub><sup>-</sup>) because of its greater asymmetry and higher glass transition temperature. At very high temperatures of 190 and 210 °C, the dielectric spectra of poly(4VIm<sup>+</sup>PF<sub>6</sub><sup>-</sup>) show an additional peak at lower frequency ( $10^3$ – $10^4$  Hz) that, at this time, has neither been labeled nor attributed it to any specific relaxation phenomenon. P4VIm<sup>+</sup> polymers, whose glass

transition temperatures are lower than that of P4VIm<sup>+</sup>PF<sub>6</sub><sup>-</sup>, do not show this lower frequency peak.

Plots of  $\tan \delta$  versus frequency for P4VIm<sup>+</sup>C<sub>2</sub>N<sub>3</sub><sup>-</sup> and P4VIm<sup>+</sup>BF<sub>4</sub><sup>-</sup> are displayed in Figures 8 and 9. The  $\tan \delta$  versus frequency plots for P4VIm<sup>+</sup>CF<sub>3</sub>SO<sub>3</sub><sup>-</sup>, BF<sub>4</sub><sup>-</sup>, TFSI<sup>-</sup>, and C<sub>2</sub>N<sub>3</sub><sup>-</sup> are similar to that for the PF<sub>6</sub><sup>-</sup> salt in that  $\alpha$  (lower temperature/higher frequency) and  $\alpha'$  (higher temperature/lower frequency) relaxation peaks were generally observed.

In order to garner some insight into the nature of the relaxation peaks, an Arrhenius analysis was used as an approximation to allow an estimate of the activation energy to be made. The log of the maxima in each relaxation peak in the PF<sub>6</sub><sup>-</sup> spectra were thus plotted against the reciprocal of the

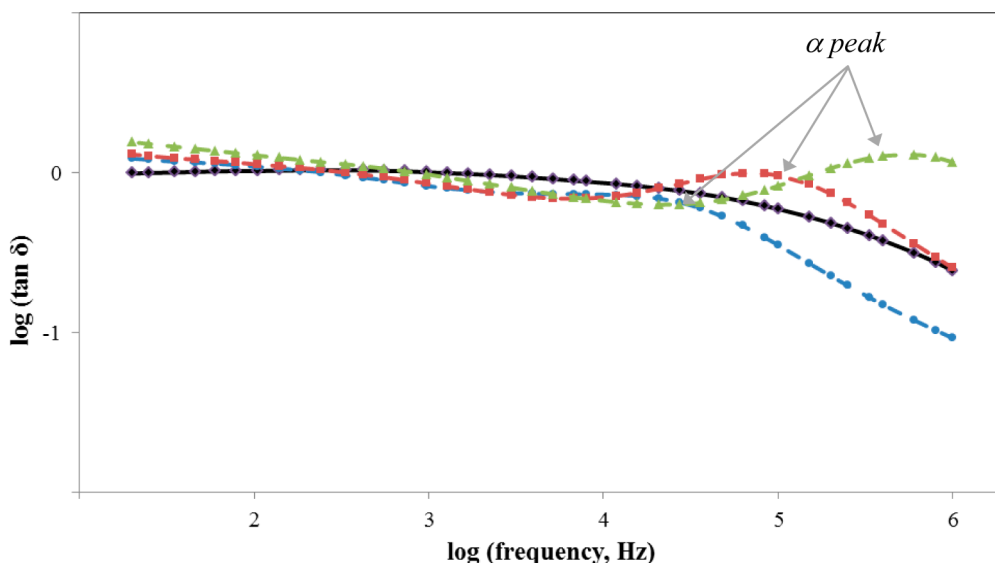


**Figure 8.** Plot of  $\tan \delta$  versus frequency: P4VIm<sup>+</sup>C<sub>2</sub>N<sub>3</sub><sup>-</sup>. Data points of different shape and color connected by solid or dashed lines of the same color are measured data at different temperatures:  $\blacklozenge$  black solid, 90 °C;  $\bullet$  blue dashed, 110 °C;  $\blacksquare$  red dashed, 130 °C;  $\blacktriangle$  green dashed, 150 °C.

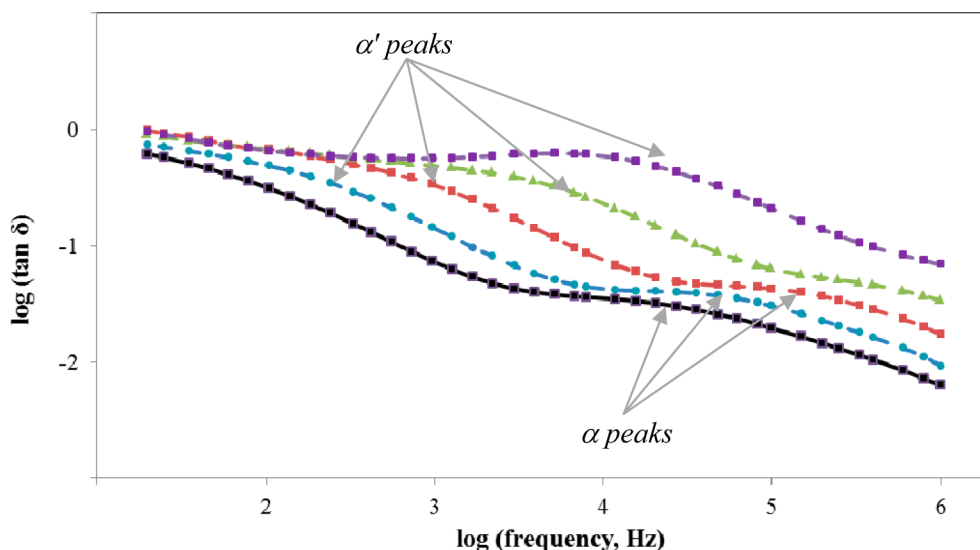


**Figure 9.** Plot of  $\tan \delta$  versus frequency: P4VIm<sup>+</sup>BF<sub>4</sub><sup>-</sup>. Data points of different shape and color connected by solid or dashed lines of the same color are measured data at different temperatures:  $\blacksquare$  black solid, 90 °C;  $\bullet$  blue dashed, 110 °C;  $\blacksquare$  red dashed, 130 °C;  $\blacktriangle$  green dashed, 150 °C;  $\blacksquare$  purple dashed, 170 °C.

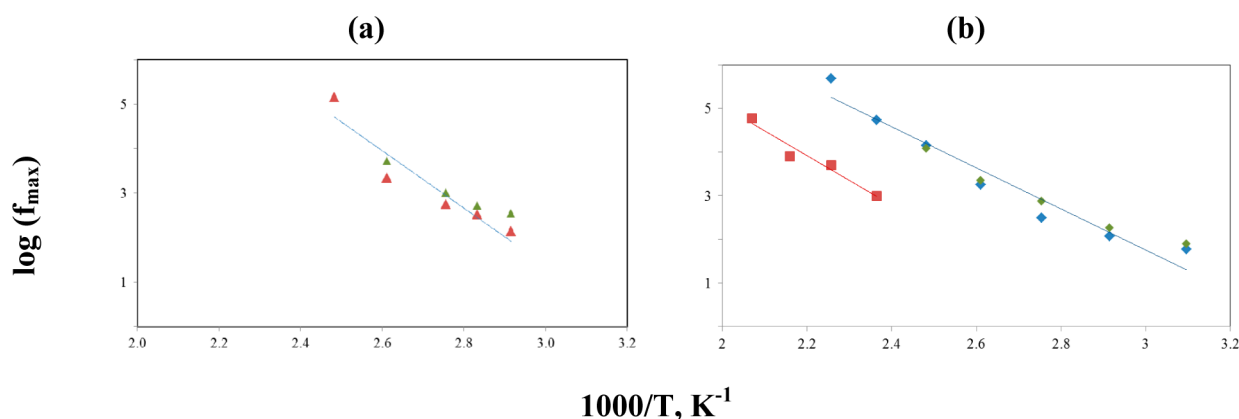
temperature,  $T$ , in kelvin. Arrhenius plots for the  $\alpha$ -relaxation (observed in Figures 7c,e) and the  $\alpha$ - and  $\alpha'$ -relaxations (observed in Figures 7d,f) are presented in Figures 10a,b. The plots displayed in Figure 10a,b include a least-squares fit line that, over the temperature range (303–483 K) at which measurements were taken, is a good fit to the data (correlation coefficients = 0.94 and 0.95, respectively, for the  $\alpha$  and  $\alpha'$  relaxation data, in Figure 10 b).

Table 2 presents fitting parameters,  $\Delta\epsilon$  (dielectric relaxation strength) and  $\sigma_0$  (dc conductivity), for the  $\alpha$ - and  $\alpha'$ -relaxations in P4VIm<sup>+</sup>PF<sub>6</sub><sup>-</sup> and P4VIm<sup>+</sup>BF<sub>4</sub><sup>-</sup>. The high-temperature, low-frequency data may have large errors in the fit parameters because of the strong conduction effect and weak relaxation peak seen there. The  $\alpha'$ -relaxation is “stronger” than  $\alpha$  in P4VIm<sup>+</sup>PF<sub>6</sub><sup>-</sup> and in P4VIm<sup>+</sup>BF<sub>4</sub><sup>-</sup>. The  $\Delta\epsilon$  values for  $\alpha'$  increase with increasing temperature in both materials; however, the  $\alpha$  process has a much weaker temperature

dependence than  $\alpha'$ , especially in P4VIm<sup>+</sup>PF<sub>6</sub><sup>-</sup>. The increase in relaxation strength with temperature for the  $\alpha$ - and  $\alpha'$ -relaxations is not expected for a segmental mode relaxation. The conductivity increases with temperature by several orders of magnitude in P4VIm<sup>+</sup>PF<sub>6</sub><sup>-</sup> but increases only slightly in P4VIm<sup>+</sup>BF<sub>4</sub><sup>-</sup>.

Fragiadakis et al.<sup>46</sup> studied a system of more conventional copolymer ionomers and report that large values of the dielectric increment may be associated with ion motion. Indeed, for the  $\alpha'$ -relaxation,  $\Delta\epsilon$  values range from 30 to 890 for P4VIm<sup>+</sup>PF<sub>6</sub><sup>-</sup> and from 28 to 92 for P4VIm<sup>+</sup>BF<sub>4</sub><sup>-</sup>. Accordingly, the  $\alpha$ - and  $\alpha'$ -relaxations are most likely attributable to ion-pair motion, with the onset of segmental motion perhaps being correlated with ion-pair motion. Plots of  $\Delta\epsilon$  vs temperature are included in the Supporting Information.

In any discussion of the origin of relaxation peaks in the dielectric spectra of ionic polymers one is obligated to consider



**Figure 10.** Frequency-max versus  $1/T$  (K): (a) P4VIm<sup>+</sup> PF<sub>6</sub><sup>-</sup> (green ▲,  $\alpha$ -relaxation, data from  $\tan \delta$  plots; red ▲,  $\alpha$ -relaxation, data from deconvoluted  $\epsilon''$  vs frequency plots); (b) P4VIm<sup>+</sup>PF<sub>6</sub><sup>-</sup> (green ◆,  $\alpha$ -relaxation, from  $\tan \delta$ ; blue ◆,  $\alpha$ -relaxation, from deconvoluted  $\epsilon''$ ); P4VIm<sup>+</sup>PF<sub>6</sub><sup>-</sup> (red ■,  $\alpha'$ -relaxation, from  $\tan \delta$ ). Points refer to measured data. Lines are least-squares fit to  $f_{\max}$  data from deconvoluted  $\epsilon''$  plots.

**Table 2.** Temperature Dependence of Conductivity,  $\sigma_0$ , and Relaxation Strength,  $\Delta\epsilon$ , for the  $\alpha$ - and  $\alpha'$ -Processes in P4VIm<sup>+</sup>PF<sub>6</sub><sup>-</sup> and P4VIm<sup>+</sup>BF<sub>4</sub><sup>-</sup>

polymer	$T$ (K)	$\Delta\epsilon(\alpha)$	$\Delta\epsilon(\alpha')$	$\sigma_0$ (S/cm)
P4VIm <sup>+</sup> PF <sub>6</sub> <sup>-</sup>	343	5.1		$2.8 \times 10^{-11}$
	363	5.7		$9.9 \times 10^{-10}$
	383	8.0		$2.3 \times 10^{-8}$
	403	7.3		$6.1 \times 10^{-8}$
	423	8.1	30	$2.0 \times 10^{-7}$
	443	7.1	74	$4.0 \times 10^{-7}$
	463	96	890	$1.4 \times 10^{-6}$
P4VIm <sup>+</sup> BF <sub>4</sub> <sup>-</sup>	363	2.4		$8.1 \times 10^{-9}$
	383	3.2	28	$2.9 \times 10^{-8}$
	403	2.8	46	$4.7 \times 10^{-8}$
	423	3.2	51	$5.2 \times 10^{-8}$
	443	4.8	92	$7.1 \times 10^{-8}$

the possibility of ion aggregation. Ion aggregates would be most expected in the triflate system in which the anion is “hard”, i.e., not highly polarizable. “Soft” anions like TFSI and dicyanamide would be least likely to suffer from ion aggregation. The similarity of dielectric spectral characteristics across the series of ion-exchanged P4VIm<sup>+</sup> salts leads us to conclude that the impact of ion aggregation and any consequent interfacial polarization peaks is minimal in the P4VIm<sup>+</sup> salt system. While X-ray diffraction or viscoelastic studies which could rule out ion aggregation have not yet been carried out in our P4VIm<sup>+</sup> system, the recent viscoelastic study by Nakamura et al.,<sup>26</sup> indicating the absence of ion aggregates in poly(1-vinyl-3-butylimidazolium salts), supports the probability that ion aggregation is not a factor in any features of the dielectric spectra of the P4VIm<sup>+</sup> salts.

Arrhenius plots of frequency versus  $1/T$  (K) for  $\alpha$ - and  $\alpha'$ -processes in the triflate, tetrafluoroborate, trifluoromethylsulfonylimide, and dicyanamide salts are indicative of greater differences in activation energy than for the  $\alpha$ - and  $\alpha'$ -processes in the PF<sub>6</sub><sup>-</sup> derivatives. Activation energies were calculated from the slope of the plots of frequency vs  $1/T$  (K) for five 4-vinylimidazolium polymer salts (CF<sub>3</sub>SO<sub>3</sub><sup>-</sup>, BF<sub>4</sub><sup>-</sup>, PF<sub>6</sub><sup>-</sup>, C<sub>2</sub>N<sub>3</sub><sup>-</sup>, and TFSI<sup>-</sup>). These data are presented in Table 3. An important finding is that the activation energy of the  $\alpha$ -relaxation appears to scale with the glass transition temperature, with  $E_a$ - $\alpha$  being lowest for the TFSI<sup>-</sup> and C<sub>2</sub>N<sub>3</sub><sup>-</sup> salts. The activation energy of the  $\alpha'$ -relaxation process was variable; however, it was highest

**Table 3.**  $E_a$  of  $\alpha$ - and  $\alpha'$ -Relaxations in P4VIm<sup>+</sup> Salts

P4VIm <sup>+</sup>	$E_a$ (kJ/mol), $\alpha$ -relaxation	$E_a$ (kJ/mol), $\alpha'$ -relaxation	heating cycle $T_g$ -mid, °C
BF <sub>4</sub> <sup>-</sup>	72	28	186
PF <sub>6</sub> <sup>-</sup>	83 <sup>a</sup>	109	200
CF <sub>3</sub> SO <sub>3</sub> <sup>-</sup>	40	18	213
C <sub>2</sub> N <sub>3</sub> <sup>-</sup>	31 <sup>b</sup>	102	88
TFSI <sup>-</sup>	28	141	81

<sup>a</sup> $E_a$  of P1VIm<sup>+</sup>PF<sub>6</sub><sup>-</sup> = 107 kJ/mol. <sup>b</sup> $E_a$  of P1VIm<sup>+</sup>C<sub>2</sub>N<sub>3</sub><sup>-</sup> = 12 kJ/mol.

in the TFSI<sup>-</sup> and C<sub>2</sub>N<sub>3</sub><sup>-</sup> salts and lowest with the CF<sub>3</sub>SO<sub>3</sub><sup>-</sup> and BF<sub>4</sub><sup>-</sup> salts. The differences between the activation energies of the  $\alpha$ - and  $\alpha'$ -processes were least pronounced in P4VIm<sup>+</sup>PF<sub>6</sub><sup>-</sup> and P4VIm<sup>+</sup>CF<sub>3</sub>SO<sub>3</sub><sup>-</sup>. The activation energies of the  $\alpha$ -relaxation process in P4VIm<sup>+</sup>PF<sub>6</sub><sup>-</sup> and P4VIm<sup>+</sup>C<sub>2</sub>N<sub>3</sub><sup>-</sup> are similar to those in P1VIm<sup>+</sup>PF<sub>6</sub><sup>-</sup> and P1VIm<sup>+</sup>C<sub>2</sub>N<sub>3</sub><sup>-</sup>. These differences in the apparent activation energies of the  $\alpha$ - and  $\alpha'$ -relaxation processes may be related to how tightly the anion is coupled to the imidazolium cation.

In light of the substantial difference in the activation energies of the  $\alpha$ - and  $\alpha'$ -relaxations of the P4VIm<sup>+</sup>C<sub>2</sub>N<sub>3</sub><sup>-</sup> and P4VIm<sup>+</sup>TFSI<sup>-</sup>, one might speculate these large soft (highly polarizable) anions are not tightly coupled and that the nature of the ion-pair motion associated with  $\alpha$ - and  $\alpha'$ -relaxations are inverted with the  $\alpha$ -relaxation being more reflective of ion-pair motion preceding segmental motion.

Agapov and Sokolov<sup>47</sup> have proposed that, in some glass-forming systems, ion diffusion can be decoupled from structural relaxation, with the extent of decoupling being characterized by the deviation of the temperature dependence of the characteristic structural relaxation time,  $\tau$ , from a simple Arrhenius behavior. This deviation can be uniquely captured in the fragility index,  $m$  (a measure of the steepness of the temperature dependence of  $\tau$  at the glass transition temperature,  $T_g$ ).<sup>48</sup> At this juncture, the molecular origins of the relaxation processes in 4-vinylimidazolium polymer salts and the degree of correlation between anion mobility and the glass transition can only be unequivocally elucidated by more extensive dielectric relaxation studies over a broader temperature range. While such measurements are planned, the present work represents a significant body of new data on the glass transition and dielectric relaxation characteristics of families of poly(1-ethyl-3-methyl-4-vinylimidazolium) and poly(3-ethyl-1-vinylimidazolium) salts.

## SUMMARY AND CONCLUSIONS

A robust process for the synthesis of 1-ethyl-3-methyl-4-vinylimidazolium triflate ( $\text{EM-4-VIm}^+\text{CF}_3\text{SO}_3^-$ ) was developed. This new monomer was synthesized in a pure, dry (water-free) state by direct alkylation of 1-methyl-5-vinylimidazole in  $\text{CH}_2\text{Cl}_2$  or ethyl acetate solution with ethyl triflate at 0 °C. While the monomer tends to polymerize spontaneously at ambient temperature or when exposed to water, it can be stored and handled without polymerization as long as it is kept dry in its crystalline state and held at temperatures below 0 °C.  $\text{EM-4-VIm}^+\text{CF}_3\text{SO}_3^-$  is readily polymerized with a free-radical initiator, and the resulting polymer has been ion-exchanged to create a family of 4-vinylimidazolium polymers in which the counterion ranged from  $\text{BF}_4^-$ ,  $\text{PF}_6^-$ , and  $\text{AsF}_6^-$  to dicyanamide ( $\text{C}_2\text{N}_3^-$ ), bistrifluoromethylsulfonamide ( $\text{TFSI}^-$ ), and triflate ( $\text{CF}_3\text{SO}_3^-$ ).

This same process was employed in the synthesis of 3-ethyl-1-vinylimidazolium triflate ( $\text{1-VIm}^+\text{CF}_3\text{SO}_3^-$ ) and its subsequent polymerization and ion exchange.

The trends in the glass transition characteristics of the various 4-vinylimidazolium and 1-vinylimidazolium polymers were similar; however, the glass transition temperatures of  $\text{P4VIm}^+\text{BF}_4^-$ ,  $\text{PF}_6^-$ ,  $\text{AsF}_6^-$ , and  $\text{CF}_3\text{SO}_3^-$  salts were significantly higher than those of the corresponding poly(1-vinylimidazolium) salts. This difference and the increase in  $T_g$  in going from  $\text{BF}_4^-$  to  $\text{AsF}_6^-$  in the 4-vinylimidazolium series were attributed to enhanced intramolecular bridging between imidazolium moieties positioned 1,3 or 1,5 along the polymer chain.

In the 30–210 °C temperature range, the dielectric relaxation spectra of the 4-vinylimidazolium polymer salts exhibited two relaxation modes. The 1-vinylimidazolium polymer salt exhibited only one relaxation mode in that temperature range. The single mode appears to correspond to the  $\alpha$ -relaxation peak, assigned to ion-pair motion in  $\text{P1VIm}^+\text{TFSI}^-$  by Nakamura et al.<sup>25</sup> The second relaxation peak, which is apparent at lower frequency in the dielectric spectra of the 4-vinylimidazolium polymer salts, was identified in this work as the  $\alpha'$ -relaxation and is also associated with ion-pair motion. The activation energy of the  $\alpha$ -relaxation in  $\text{P4VIm}^+\text{BF}_4^-$ ,  $\text{PF}_6^-$ ,  $\text{CF}_3\text{SO}_3^-$ ,  $\text{TFSI}^-$ , and  $\text{C}_2\text{N}_3^-$  salts ranged from 83 to 28 kJ/mol. The activation energy of the  $\alpha$ -relaxation in poly(4-vinylimidazolium  $\text{TFSI}^-$  and  $\text{C}_2\text{N}_3^-$ ) was lowest, ranging from 31 to 28 kJ/mol. The activation energy of the  $\alpha$ -relaxation in  $\text{P4VIm}^+$  salts appears to scale with the glass transition temperature of the various salts. The activation energy of the  $\alpha'$ -relaxation in  $\text{P4VIm}^+\text{TFSI}^-$  and  $\text{C}_2\text{N}_3^-$  (141 and 102 kJ/mol), respectively, was dramatically higher than that for the  $\alpha$ -relaxation (28 and 31 kJ/mol, respectively).

## ASSOCIATED CONTENT

### Supporting Information

DSC thermograms for all poly(4-vinylimidazolium salts) and dielectric results on  $\text{TFSI}^-$  salts of 1-vinyl- and 4-vinylimidazolium polymers which correlates the present results with data reported by Nakamura et al.<sup>24</sup> on poly(3-ethyl-1-vinylimidazolium  $\text{TFSI}^-$ ); plots of  $\Delta\epsilon$  vs temperature. This material is available free of charge via the Internet at <http://pubs.acs.org>.

## AUTHOR INFORMATION

### Corresponding Author

\*E-mail [twssch@rit.edu](mailto:twssch@rit.edu).

### Notes

The authors declare no competing financial interest.

## ACKNOWLEDGMENTS

This research was enabled and supported by the National Science Foundation. Work at RIT and Tufts was funded by DMR-0938957 and DMR-0906455, respectively. This support is gratefully acknowledged.

## REFERENCES

- (1) Fericola, A.; Scrosati, B.; Ohno, H. Potentialities of ionic liquids as new electrolyte media in advanced electrochemical devices. *Ionics* **2006**, *12*, 95–102.
- (2) Hayashi, K.; Yasue Nemoto, Y.; Akuto, K.; Sakurai, Y. Ionic liquids for lithium secondary batteries. *NTT Tech. Rev.* **2004**, *2* (9), 48–54.
- (3) Martinelli, A.; Matic, A.; Jacobsson, P.; Borjesson, L.; Fericola, A.; Panero, S.; Scrosati, B.; Ohno, H. Physical properties of proton conducting membranes based on a protic ionic liquid. *J. Phys. Chem. B* **2007**, *111*, 12462–12467.
- (4) Stenger-Smith, J. D.; Webber, C. K.; Anderson, N.; Chafin, A. P.; Zong, K.; Reynolds, J. Poly(3,4-alkylenedioxythiophene)-based supercapacitors using ionic liquids as supporting electrolytes. *J. Electrochem. Soc.* **2002**, *148* (8), A973–A977.
- (5) Wang, P.; Zakeeruddin, S. M.; Humphry-Baker, R.; Grätzel, M. A binary ionic liquid electrolyte to achieve  $\geq 7\%$  power conversion efficiencies in dye-sensitized solar cells. *Chem. Mater.* **2004**, *16*, 2694–2696.
- (6) Scott, M. P.; Rahman, M.; Brazel, C. S. Application of ionic liquids as low-volatility plasticizers for PMMA. *Eur. Polym. J.* **2003**, *39* (10), 1947–1953.
- (7) Susan, Md. A. B. H.; Kaneko, T.; Noda, A.; Watanabe, M. *J. Am. Chem. Soc.* **2005**, *127*, 4976.
- (8) Snedden, P.; Cooper, A. I.; Scott, K.; Winterton. Cross-linked polymer/ionic liquid composite materials. *Macromolecules* **2003**, *36*, 4549–4556.
- (9) Vidal, F.; Juger, J.; Chevrot, C.; Teyssié. Interpenetrating polymer networks from polymeric imidazolium-type ionic liquid and polybutadiene. *Polym. Bull.* **2006**, *57* (4), 1436–2449.
- (10) Yeon, S.-H.; Kim, K.-S.; Choi, S.; Cha, J.-H.; Lee, H. Characterization of PVdF(HFP) gel electrolytes based on 1-(2-hydroxyethyl)-3-methyl imidazolium ionic liquids. *J. Phys. Chem. B* **2005**, *109* (38), 17928–17935.
- (11) Sutto, T. E.; De Long, H. C.; Trulove, P. C. Physical properties of substituted imidazolium based ionic liquids gel electrolytes. *Z. Naturforsch.* **2002**, *57A*, 839–846.
- (12) Fuller, J.; Breda, A. C.; Carlin, R. T. Ionic liquid-polymer gel electrolytes. *J. Electrochem. Soc.* **1997**, *144* (4), L67–L70.
- (13) Shahin, M.; Kim, K. J.; Leo, D. J. Ionic polymer-metal composites as multifunctional materials. *Polym. Compos.* **2004**, *24* (1), 24–33.
- (14) Lee, J.; Panzer, M. J.; He, Y.; Lodge, T. P.; Frisbie, D. Ion gated polymer thin-film transistors. *J. Am. Chem. Soc.* **2007**, *129*, 4532–4533.
- (15) Lu, W.; Fadeev, A. G.; Qi, B.; Mattes, B. R. Fabricating conducting polymer electrochromic devices using ionic liquids. *J. Electrochem. Soc.* **2004**, *151* (2), H33–H39.
- (16) Marcella, R.; Alcaide, F.; Sardon, H.; Pomposo, J. A.; Pozo-Gonzalo, C.; Mecerreyes, D. Tailor-made polymer electrolytes based upon ionic liquids and their application in all-plastic electrochromic devices. *Electrochem. Commun.* **2006**, *8* (3), 482–488.
- (17) Mecerreyes, D. Polymeric ionic liquids: Broadening the properties and applications of polyelectrolytes. *Prog. Polym. Sci.* **2011**, *36*, 1629–1648.

- (18) Green, O.; Grubjesic, S.; Lee, S.; Firestone, M. A. The design of polymeric ionic liquids for the preparation of functional. *J. Macromol. Sci., Part C: Polym. Rev.* **2009**, *49*, 339–360.
- (19) Gibson, H. W. Perspective for a special issue of polymer reviews on: ionic liquids and their derivatives in polymer science and engineering. *J. Macromol. Sci., Part C: Polym. Rev.* **2009**, *49*, 289–290.
- (20) Green, M. D.; Long, T. E. Designing imidazole-based ionic liquids and ionic liquid monomers for emerging technologies. *J. Macromol. Sci., Part C: Polym. Rev.* **2009**, *49*, 291–314.
- (21) Chen, H.; Choi, J.-H.; Salas-de la Cruz, D.; Winey, K. I.; Elabd, Y. A. Polymerized ionic liquids: the effect of random copolymer composition on ion conduction. *Macromolecules* **2009**, *42*, 4809–4816.
- (22) Watanabe, M.; Yamada, S.-I.; Ogata, N. Ionic conductivity of polymer electrolytes containing room temperature molten salts based on pyridinium halide and aluminum chloride. *Electrochim. Acta* **1995**, *40* (13–14), 2285–2288.
- (23) Ye, Y.; Elabd, Y.; Yossef, A. Anion exchanged polymerized ionic liquids: High free volume single ion conductors. *Polymer* **2011**, *52*, 1309–1317.
- (24) Nakamura, K.; Saiwaki, T.; Fukao, K. Dielectric relaxation behavior of polymerized ionic liquid. *Macromolecules* **2010**, *43*, 6092–6098.
- (25) Nakamura, K.; Saiwaki, T.; Fukao, K.; Inoue, T. Viscoelastic behavior of the polymerized ionic liquid poly[1-ethyl-3-vinylimidazolium bis(trifluoromethanesulfonylimide)]. *Macromolecules* **2011**, *44*, 7719–7726.
- (26) Nakamura, K.; Fukao, K.; Inoue, T. Dielectric relaxation and viscoelastic behavior of polymerized ionic liquids with various counteranions. *Macromolecules* **2012**, *45*, 3850–3858.
- (27) Havriliak, S.; Negami, S. A complex plane representation of dielectric and mechanical relaxation processes in some polymers. *Polymer* **1967**, *8*, 161. Havriliak, S.; Negami, S. *J. Polym. Sci., Part C* **1966**, *16*, 99.
- (28) Kremer, F.; Schonhals, A. *Broadband Dielectric Spectroscopy*; Springer: Berlin, Germany, 2002.
- (29) Overberger, C. G.; Glowaky, R. C.; Pacansky, T. J.; Sannes, K. N. *Macromol. Synth.* **1974**, *5*, 43–49.
- (30) Overberger, C. G.; Kawakami, Y. Esterolytic activity of imidazole-containing polymers. Synthesis and characterization of copoly[1-alkyl-4- or 5-vinylimidazole/4(5)-vinylimidazole] and its catalytic activity in the hydrolysis of p-nitrophenyl acetate. *J. Polym. Sci., Polym. Chem. Ed.* **1978**, *16*, 1237–1248.
- (31) Wang, J.; Smith, T. W. *Polym. Prepr.* **2004**, *45* (2), 290–291.
- (32) Salamone, J. C.; Snider, B.; Fitch, W. L. Polymerization of 4-vinylpyridinium salts. III A clarification of the mechanism of spontaneous polymerization. *J. Polym. Sci., Part A-1* **1971**, *9*, 1493–1504.
- (33) Fife, W. K.; Ranganathan, P.; Zeldin, M. A general synthesis of 1-alkyl-4-vinylpyridinium ions. Alkylation of 4-vinylpyridine with primary alkyl triflates. *J. Org. Chem.* **1990**, *55*, 5610–5613.
- (34) Hirao, M.; Ito, K.; Ohno, H. Preparation and polymerization of new organic molten salts; N-alkylimidazolium salt derivatives. *Electrochim. Acta* **2000**, *45*, 1291–1294.
- (35) Marcilla, R.; Blazquez, A. J.; Rodriguez, J.; Pomposo, J. A.; Mecerreyes, D. Tuning the solubility of polymerized ionic liquids by simple anion-exchange reactions. *J. Polym. Sci., Part A: Polym. Chem.* **2003**, *42*, 208–212.
- (36) Marcilla, R.; Blazquez, A. J.; Fernandez, R.; Grande, H.; Pomposo, J. A.; Mecerreyes, D. Synthesis of novel polycations using the chemistry of ionic liquids. *Macromol. Chem. Phys.* **2005**, *206*, 299–304.
- (37) Vygodskii, Ya. S.; Melnik, O. A.; Shaplov, A. S. E.; Lozinskaya, I.; Malyshkina, I. A.; Gavrilova, N. D. Synthesis and ionic conductivity of polymer ionic liquids. *Polym. Sci., Ser. A* **2007**, *49* (3), 256–261.
- (38) Jenkins, H. D. B.; Roobottom, H. K.; Passmore, J.; Glasser, L. *Inorg. Chem.* **1999**, *38*, 3609–3620.
- (39) Eisenberg, A. Glass transitions in ionic polymers. *Macromolecules* **1971**, *4*, 125–129.
- (40) Tsutsui, T.; Tanaka, T. Role of electrostatic forces in the glass transition temperatures of ionic polymers. *Polymer* **1977**, *18*, 817.
- (41) Agapov, A. Decoupling phenomena in dynamics of soft matter. Dissertation presented to the Graduate Faculty of the University of Akron, Dec 2011.
- (42) Gabbott, P. A Practical Introduction to Differential Scanning Calorimetry. In *Principles and Application of Thermal Analysis*; Gabbott, P., Ed.; Blackwell Publishing Ltd.: Oxford, 2008.
- (43) DSC data for all poly(1-ethyl-3-methyl-4-vinylimidazolium salts) can be view in the Supporting Information.
- (44) Benson, S. W. *Thermochemical Kinetics*, 2nd ed.; Wiley-Interscience: New York, 1976.
- (45) Dielectric data ( $\epsilon''$  versus frequency) obtained in our laboratories at 50 and 90 °C for poly(3-ethyl-1-vinylimidazolium TFSI) and poly(1-ethyl-3-methyl-4-vinylimidazolium TFSI) were correlated with dielectric results reported by Nakamura et al. Data points were digitized from Nakamura's plot of ( $\epsilon''$  versus angular frequency,  $\omega$ ) for poly(3-ethyl-1-vinylimidazolium TFSI) at 40 and 90 °C. That information is provided in the Supporting Information.
- (46) Fragiadakis, D.; Dou, S.; Colby, R. H.; Runt, J. Molecular mobility and Li<sup>+</sup> conduction in polyester copolymer ionomers based on poly(ethylene oxide). *J. Chem. Phys.* **2009**, *130*, 064907.
- (47) Agapov, A. L.; Sokolov, A. P. Decoupling ionic conductivity from structural relaxation: A way to solid polymer electrolytes? *Macromolecules* **2011**, *44*, 4410–4414.
- (48) Kunal, K.; Robertson, C. G.; Pawlus, S.; Hahn, S. F.; Sokolov, A. P. Role of chemical structure in fragility of polymers: a qualitative picture. *Macromolecules* **2008**, *41*, 7232–7238.